Optical interband transitions in [111] poled relaxor-based ferroelectric $0.24Pb(In_{1/2}Nb_{1/2})O_3$–$(0.76 - x)Pb(Mg_{1/3}Nb_{2/3})O_3$–$xPbTiO_3$ single crystal

Fengmin Wu, Bin Yang, Enwei Sun, Zhu Wang, Yongqi Yin, Yanbo Pei, Wenlong Yang & Wenwu Cao

Journal of Materials Science
Full Set - Includes `Journal of Materials Science Letters'

ISSN 0022-2461
Volume 47
Number 6

J Mater Sci (2012) 47:2818-2822
DOI 10.1007/s10853-011-6110-7

Springer

J Mater Sci (2012) 47:2818–2822
DOI 10.1007/s10853-011-6110-7

Optical interband transitions in [111] poled relaxor-based ferroelectric $0.24Pb(In_{1/2}Nb_{1/2})O_3$–$(0.76 - x)Pb(Mg_{1/3}Nb_{2/3})O_3$–$xPbTiO_3$ single crystal

Fengmin Wu · Bin Yang · Enwei Sun · Zhu Wang · Yongqi Yin · Yanbo Pei · Wenlong Yang · Wenwu Cao

Received: 26 August 2011 / Accepted: 5 November 2011 / Published online: 18 November 2011

Abstract Optical transmission spectra of single crystal $0.24Pb(In_{1/2}Nb_{1/2})O_3$–$(0.76 - x)Pb(Mg_{1/3}Nb_{2/3})O_3$–$xPbTiO_3$ ($x = 0.27$, 0.33) were measured in the pseudo-cubic crystallographic directions [111] and [11$\bar{2}$]. Ferroelectric domain structures were observed in order to explain the difference of transmittance for the two composition crystals. Wavelength dependence of the absorption coefficients was measured and the optical energy band gaps were calculated for both direct and indirect transitions, which are $E_{gd} = 3.09$–3.18 eV and $E_{gi} = 2.89$–2.96 eV, respectively, and the phonon energy is $E_p = 0.07$–0.08 eV. The transmission spectra were explained by the refractive indices and extinction coefficients measured by spectroscopic ellipsometry.

Introduction

Relaxor-based ferroelectric single crystals $(1 - x)Pb(Mg_{1/3}Nb_{2/3})O_3$–$xPbTiO_3$ (PMN–PT) with compositions near the morphotropic phase boundary (MPB) have been extensively studied due to their extraordinary large electromechanical coupling coefficients ($k_{33} > 90\%$), piezoelectric coefficients ($d_{33} = 1500$–2500 pC/N), and excellent optical properties[1–3]. However, their relatively low Curie temperatures (130–170 °C) and low rhombohedral to tetragonal phase transition temperature (50–100 °C) lead to unsatisfactory temperature stability and low coercive field, which limit their potential applications. The ternary $xPb(In_{1/2}Nb_{1/2})O_3$–$(1\text{-}x\text{–}y)Pb(Mg_{1/3}Nb_{2/3})O_3$–$yPbTiO_3$ (PIN–PMN–PT) single crystal system has about 30 °C higher rhombohedral–tetragonal phase transition temperature and 2.5 times lager coercive field compared with that of PMN–PT single crystals. More importantly, they have just as excellent piezoelectric properties as that of PMN–PT single crystals [4–9].

Although the dielectric and piezoelectric properties of PIN–PMN–PT have been studied by many researchers, the basic optical properties of PIN–PMN–PT single crystals, such as optical transmittance, refractive indices, and extinction coefficients, have not been investigated. The studies on optical band gaps and electronic transitions during the optical absorption process are of great interest for potential applications in optic devices and for answering some basic physics questions on the energy levels of these relaxor-based ferroelectric single crystals.

More recently, it was found that the [111] poled 0.24PIN–0.49PMN–0.27PT single crystal has stable single domain state under natural conditions, which can greatly enhance the optical transmittance of the crystal [10]. In addition, it is known that the [111] poled binary PMN–0.33PT single crystal (MPB composition) has excellent optical and electro-optic properties, such as very high effective electro-optic coefficient, $r_c = 109$ pm/V [11]. Hence, ternary PIN–PMN–0.33PT with MPB composition is also expected to have good electro-optic properties. In this study, the optical transmittance spectra were measured

F. Wu · B. Yang · E. Sun · Z. Wang · Y. Yin · Y. Pei · W. Yang · W. Cao
Condensed Matter Science and Technology Institute, Harbin Institute of Technology, Harbin 150080, China
e-mail: binyang@hit.edu.cn

F. Wu
College of Applied Science, Harbin University of Science and Technology, Harbin 150080, China

W. Cao (✉)
Materials Research Institute, The Pennsylvania State University, University Park, PA 16802, USA
e-mail: dzk@psu.edu

along the pseudo-cubic crystallographic directions [111] and [11$\bar{2}$] for poled 0.24PIN–(0.76 − x)PMN–xPT with $x = 0.27$ and 0.33. The band gaps were obtained for both direct and indirect transitions from the optical spectra measurements. We have also observed the domain structures using polarized microscopy to explain the differences of the transmittance for the two composition crystals. The refractive indices and extinction coefficients were also analyzed.

Experimental

High-quality PIN–PMN–PT single crystals used in this study for the optical transmittance, refractive index and extinction coefficient measurements were grown by the modified Bridgman method. The PIN content is insensitive to composition segregation, but the PT content along the growth direction varies due to the segregation of titanium in the crystal. Samples of desired geometries were cut from the same slice of a crystal boule to warrant composition uniformity, and the PT contents of 0.27 and 0.33 were determined based on the dielectric and piezoelectric measurements and the phase diagram. The PIN content for both crystals is 0.24. All samples were oriented by using the Laue X-ray machine with an accuracy of ±0.5° and cut along crystallographic directions $[1\bar{1}0] \times [11\bar{2}] \times [111]$ in pseudo-cubic coordinates. The samples were sputtered with gold electrodes on the [111] and $[\bar{1}\bar{1}\bar{1}]$ surfaces, and poled in silicone oil with a field of 10 kV/cm at room temperature. Then, the surfaces of the samples were polished to optical quality with the thickness of 0.6 mm. Two kinds of samples, [111] polished and [11$\bar{2}$] polished, were prepared for each PT content single crystal.

Optical transmission spectra of the [111] poled 0.24PIN–(0.76 − x)PMN–xPT, $x = 0.27$,0.33, single crystals were measured at room temperature in the wavelength range of 300–1000 nm with 1 nm interval using UV–VIS–NIR spectrophotometer (SP-752PC). The ferroelectric domain configurations of the crystals after poling were observed using polarized optical microscopy (ZEISS AXIOSKOP40). SE measurements were carried out at room temperature to measure the refractive index and extinction coefficient using a spectroscopic ellipsometer (α-SE™, J.A. Woollam Co., Inc., American).

Result and discussion

The samples are transparent in visible and near-infrared region based on the optical transmission spectra in Fig. 1, but become completely opaque at about 400 nm, which is

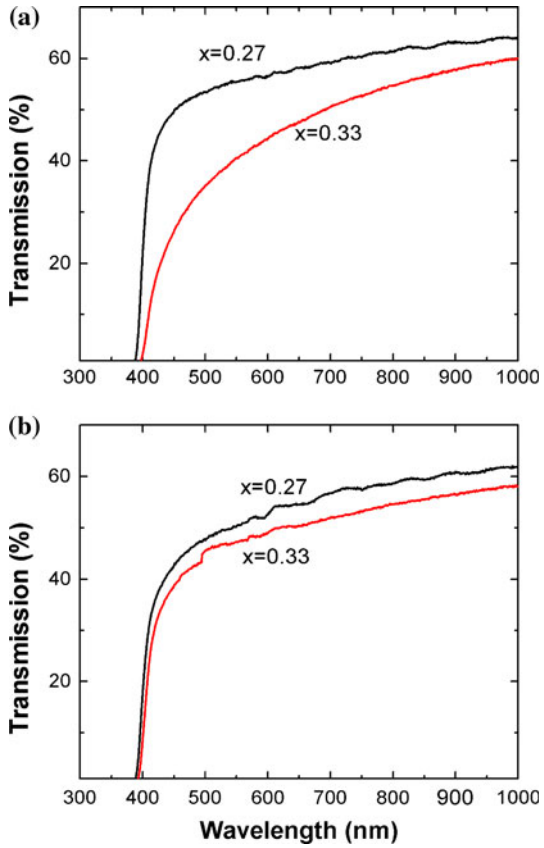

Fig. 1 The transmission characteristic in near UV and visible light region of **a** [111] and **b** [11$\bar{2}$]-oriented 0.24PIN–(0.76 − x)PMN–xPT single crystal

the optical absorption edge at UV. The transmittance of 0.24PIN–0.49PMN–0.27PT single crystal is higher than that of 0.24PIN–0.43PMN–0.33PT in both [11$\bar{2}$] and [111] directions. For the 0.24PIN–0.49PMN–0.27PT single crystal, the crystal symmetry is rhombohedral and the spontaneous polarization is along the ⟨111⟩ direction. After poling along the [111] direction, the crystal becomes single domain as shown in Fig. 2a, which appears almost extinction when observed using a polarized optical microscopy along the (111) surface. But for the 0.24PIN–0.43PMN–0.33PT single crystal with MPB composition, optical microscopy observation show the existence of monoclinic phase (usually recognized as pseudo-orthorhombic phase with the spontaneous polarization along ⟨110⟩). After poling along [111] direction, the 0.24PIN–0.43PMN–0.33PT single crystal still has multi-domain structure as shown in Fig. 2b. The stripe domain width is about 2–4 μm and the domain walls caused light scattering, which resulted in lower optical transmittance in the 0.24PIN–0.43PMN–0.33PT single crystal. In addition, the difference of the transmittance spectra between the [11$\bar{2}$] and [111] directions are small for 0.24PIN–0.49PMN–0.27PT in its single domain state. However, the optical transmittance along

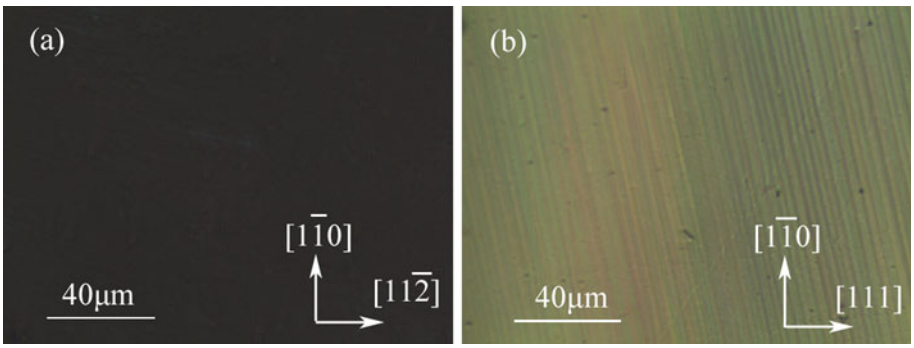

Fig. 2 Domain structures observed on (111) surface of **a** 0.24PIN–0.49PMN–0.27PT and **b** 0.24PIN–0.43PMN–0.33PT single crystal poled along [111] direction

[111] is much lower than that along [11$\bar{2}$] for the 0.24PIN–0.43PMN–0.33PT single crystal, because the orientation of the domain walls are inclined to the [1$\bar{1}$0] direction as shown in Fig. 2b. Compared with 0.24PIN–0.49PMN–0.27PT, the optical absorption edge of 0.24PIN–0.43PMN–0.33PT has a red shift. Similar phenomena had also been found in the binary relaxor-based ferroelectric PMN–*x*PT and PZN–*x*PT crystals, i.e., the optical absorption edges have red shift with increasing PT contents [12–14].

The optical absorption coefficient α can be calculated from [15]

$$\alpha = -\frac{1}{L}\ln\frac{-(1-R)^2+\sqrt{(1-R)^4+4R^2T^2}}{2R^2T}, \quad (1)$$

where T is the transmittance, R is the surface reflectivity, and L is the thickness of the sample.

For optical interband transitions, the absorption coefficient α is deemed to be zero in the near-infrared range, where T becomes a constant because of the very low photon energy. In this case, Eq. 1 reduces to $T = (1 - R)/(1 + R)$, which offered a means to derive the value of R [13].

The optical interband transitions include direct and indirect transitions because the bottom of the conduction band and top of the valance band contains more than one extrema. The optical band gaps can be estimated by the predominant mechanism of band to band transitions. In the allowed direct transition, the electrons in the valence band transit vertically to the conduction band under the excitation of photons. The absorption coefficient as a function of photon energy in the allowed direct transition can be expressed as [16]

$$\alpha = \frac{A}{h\nu}(h\nu - E_{gd})^{1/2}, \quad (2)$$

where A is a constant, ν is the frequency, h is the Planck constant, and E_{gd} is the allowed direct energy gap.

In the indirect transition, the electrons transit from the top of the valence band to the bottom of the conduction band with participation of photons and suitable phonons. In this case, the absorption coefficient can be fitted to the following formula [17]:

$$\alpha = \frac{B}{h\nu}(h\nu - E_{gi} \pm E_p)^2, \quad (3)$$

where B is another constant, E_{gi} is the indirect energy gap, and E_p is the energy of the absorbed (+) or emitted (−) phonons.

The curve of $(\alpha h\nu)^2$ versus $h\nu$ for the single domain 0.24PIN–0.49PMN–0.27PT in [111] is shown in Fig. 3 in the photon energy range from 2.90 to 3.20 eV. The direct band gap energy was determined to be $E_{gd} = 3.18$ eV by extrapolating the linear portion of the curve to zero. The dependence of $(\alpha h\nu)^{1/2}$ on $h\nu$ exhibits three distinct linear segments, similar to the characteristics of the absorption edges of other perovskite ferroelectrics [18]. The values of $E_{g1} = E_{gi} + E_p$ and $E_{g2} = E_{gi} - E_p$ were obtained to be $E_{g1} = 3.03$ eV and $E_{g2} = 2.89$ eV, respectively, by extrapolating $(\alpha h\nu)^{1/2}$ versus $h\nu$ curves to zero. Therefore, the indirect energy gap and the phonon energy can be determined to be $E_{gi} = 1/2(E_{g1} + E_{g2}) = 2.96$ eV and $E_p = 1/2(E_{g1} - E_{g2}) = 0.07$ eV, respectively. The values of direct band gap E_{gd}, indirect band gap E_{gi}, and the

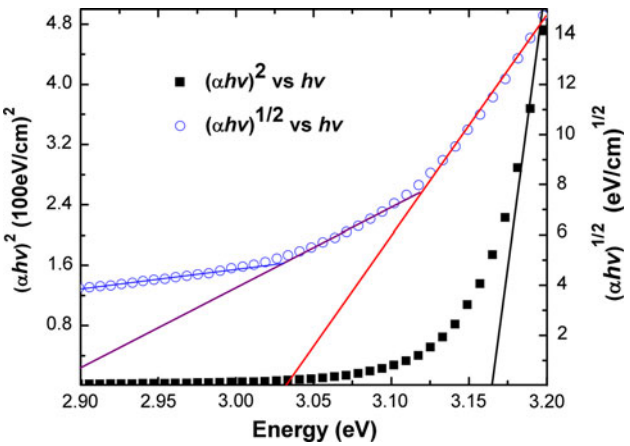

Fig. 3 Variations in $(\alpha h\nu)^2$ and $(\alpha h\nu)^{1/2}$ versus photon energy $h\nu$ for [111] poled 0.24PIN–0.49PMN–0.27PT single crystal of [111]-oriented

Table 1 The values of direct band gap E_{gd}, indirect band gap E_{gi}, and the energy of the phonon E_p for 0.24PIN–(0.76 − x)PMN–xPT single crystals along the two crystallographic directions

Material	Orientation	E_{gd} (eV)	E_{g1} (eV)	E_{g2} (eV)	E_{gi} (eV)	E_p (eV)
0.24PIN–0.49PMN–0.27PT	[111]	3.18	3.03	2.89	2.96	0.07
	[11$\bar{2}$]	3.17	3.04	2.88	2.96	0.08
0.24PIN–0.43PMN–0.33PT	[111]	3.09	2.95	2.82	2.89	0.07
	[11$\bar{2}$]	3.10	2.96	2.83	2.90	0.07

phonon energy E_p for different PT contents and different orientations are calculated and listed in Table 1. The direct energy gap E_{gd} and indirect energy gap E_{gi} of 0.24PIN–0.49PMN–0.27PT are higher than that of 0.24PIN–0.43PMN–0.33PT, and the phonon energy E_p is in the range of 0.07–0.08 eV.

It is already well known in lattice dynamic theories that the static dielectric behavior of the $A(B_1B_2)O_3$-type perovskite compounds is determined primarily by the $(B_1B_2)O_6$ oxygen-octahedral structure. For optical properties, the $(B_1B_2)O_6$ oxygen-octahedron governs the lower lying conduction bands and the upper valence bands. The B-cation d orbitals and the O-anion $2p$ orbitals associated with each octahedron are the major contributors to the energy bands of interest. Other ions contribute to higher lying conduction bands, and these bands are of negligible importance provided the electronic polarizability of these ions is small [18]. Therefore, the common $(B_1B_2)O_6$ oxygen-octahedral structure determines the basic energy levels in the crystal for the $A(B_1B_2)O_3$-type perovskite compounds. The 0.24PIN–(0.76 − x)PMN–xPT, PMN–xPT, and PZN–xPT single crystals with different compositions should have similar optical absorption edges with slight differences due to different B-site (including B_1 and B_2) cations [12]. It was found that the optical band gap energies are indeed very similar as shown in Table 2.

The refractive index and extinction coefficient of 0.24PIN–(0.76 − x)PMN–xPT, $x = 0.27$, 0.33, single crystals in [11$\bar{2}$] were measured by spectroscopic ellipsometry. Figure 4 depicts the wavelength dependence of the refractive indices n and extinction coefficients k at room temperature. The refractive indices decrease monotonically when the wavelength increases for both samples. The refractive index of $x = 0.33$ single crystal is higher than that of $x = 0.27$ single crystal due to the higher refractive index of pure PT compared with that of pure PMN [10]. The extinction coefficients also decrease with the wavelength for both samples. Because the k-values of 0.24PIN–(0.76 − x)PMN–xPT single crystals are small at the wavelength above 450 nm, they appear transparent in the visible light region [19], which is consistent with the results of the optical transmission spectra in Fig. 1. For the 0.24PIN–(0.76 − x)PMN–xPT single crystals, the main

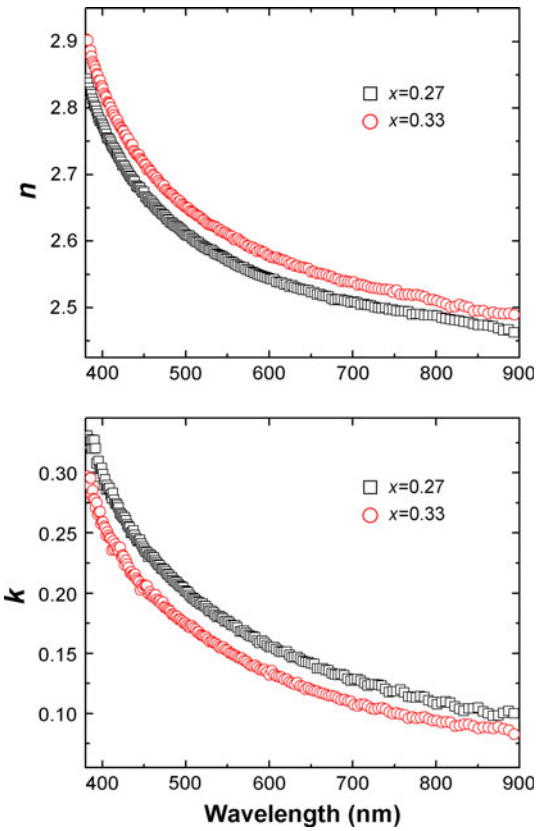

Fig. 4 Wavelength dependence of the refractive indices n and extinction coefficients k of 0.24PIN–(0.76 − x)PMN–xPT single crystal at room temperature

Table 2 The optical band gap energies of PMN–xPT and PZN–0.07PT single crystals

Material	E_{gd} (eV)
PMN–0.24PT[a]	3.24
PMN–0.30PT[a]	3.23
PMN–0.31PT[a]	3.23
PMN–0.33PT[a]	3.22
PZN–0.07PT[b]	3.144
0.24PIN–0.49PMN–0.27PT[c]	3.18
0.24PIN–0.43PMN–0.33PT[c]	3.09

[a] Reference [14]

[b] Reference [13]

[c] Present work

contribution of optical loss comes from the band gap and domain wall scattering. The rapid increase of k at the wavelength below 450 nm indicates that the optical transmission cut off is due to the absorption near the band gap.

Conclusions

Optical transmission spectra of [111] poled relaxor-based ferroelectric single crystal 0.24PIN–$(0.76 - x)$PMN–xPT, with $x = 0.27$ and 0.33, were measured in the crystallographic directions [111] and $[11\bar{2}]$. We found that the 0.24PIN–0.49PMN–0.27PT and 0.24PIN–0.43PMN–0.33PT single crystals have different domain structures and spontaneous polarization, which induce the difference in their optical transmittance. The optical energy band gaps were calculated based on the theory of band to band transitions. The direct and indirect energy gaps were determined to be $E_{gd} = 3.09$–3.18 eV and $E_{gi} = 2.89$–2.96 eV, respectively, and the phonon energy is $E_p = 0.07$–0.08 eV. The refractive indices and extinction coefficients were also measured to explain the shape of transmission spectra.

Acknowledgements This research was supported by the NIH under Grant No. P41-EB21820, the National Nature Science Foundation of China under Grant No. 10704021 and H. C. Materials Inc.

References

1. Park SE, Shrout TR (1997) J Appl Phys 82:1804
2. Zhang SJ, Luo J, Xia R, Rehrig PW, Randall CA, Shrout TR (2006) Solid State Commun 137:16
3. Damjanovic D, Budimir M, Davis M, Setter N (2006) J Mater Sci 41:65. doi:10.1007/s10853-005-5925-5
4. Hosono Y, Yamashita Y, Sakamoto H, Ichinose N (2003) Jpn J Appl Phys, Part 1 42:5681
5. Hosono Y, Yamashita Y, Hirayama K, Ichinose N (2005) Jpn J Appl Phys, Part 1 44:7037
6. Zhang S, Luo J, Hackenberger W, Shrout TR (2008) J Appl Phys 104:064106
7. Sun E, Zhang S, Luo J, Shrout TR, Cao W (2010) Appl Phys Lett 97:032902
8. Tian J, Han P, Huang X, Pan H, Carroll JF III, Payne DA (2007) Appl Phys Lett 91:222903
9. Zhang S, Luo J, Hackenberger W, Sherlock NP, Meyer RJ Jr, Shrout TR (2009) J Appl Phys 105:104506
10. Sun E, Cao W, Jiang W, Han P (2011) Appl Phys Lett 99:032901
11. Wan X, Luo H, Zhao X, Wang D, Chan HLW, Choy CL (2004) Appl Phys Lett 85:5233
12. Bing YH, Guo R, Bhalla AS (2000) Ferroelectrics 242:1
13. Sun E, Zhang R, Wang Z, Xu D, Li L, Cao W (2010) J Appl Phys 107:113532
14. Wan XM, Chan HLW, Choy CL, Zhao XY, Luo HS (2004) J Appl Phys 96:1387
15. Macfarlane GG, Mclean TP, Quarrington JE, Roberts V (1957) Phys Rev 108:1377
16. Tauc JC (1972) Optical properties of solids. North-Holland, Amsterdam
17. El-Korashy A, El-Fadl AA (1999) Phys B 271:205
18. DiDomenico M, Wemple SH (1969) J Appl Phys 40:720
19. Wan XM, Zhao XY, Chan HLW, Choy CL, Luo HS (2005) Mater Chem Phys 92:123